

# Thermal Decomposition of Methyl Phenyl Ether in Shock Waves: The Kinetics of Phenoxy Radical Reactions<sup>†</sup>

Chin-Yu Lin

Department of Chemistry, The Catholic University of America, Washington, D.C. 20064-0001

and M. C. Lin\*<sup>‡</sup>

Chemistry Division, Code 6105, Naval Research Laboratory, Washington, D.C. 20375-5000

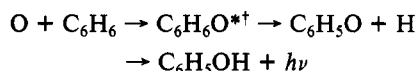
(Received: July 26, 1985)

The unimolecular decomposition of methyl phenyl ether (anisole) was studied in incident shock waves covering the temperature range from 1000 to 1580 K and the pressure range from 0.4 to 0.9 atm. The CO formed in the reaction, monitored by resonance absorption using a stabilized CW CO laser, could be satisfactorily accounted for by a four-reaction mechanism:  $C_6H_5OCH_3 \rightarrow C_6H_5O + CH_3$  (1),  $C_6H_5O \rightarrow CO + C_5H_5$  (2),  $CH_3 + C_6H_5O \rightarrow o$ - and  $p$ - $CH_3C_6H_4OH$  (3), and  $CH_3 + CH_3 \rightarrow C_2H_6$  (4). Kinetic modeling of observed CO production profiles based on the above mechanism with 70 sets of data led to  $k_1 \approx (1.2 \pm 0.3) \times 10^{16} \exp(-33\,100/T) \text{ s}^{-1}$ ,  $k_2 = 10^{11.40 \pm 0.20} \exp(-22\,100 \pm 450/T) \text{ s}^{-1}$ , and  $k_3 = (5.5 \pm 2.0) \times 10^{11} \text{ cm}^3 \cdot \text{mol}^{-1} \cdot \text{s}^{-1}$ . The relatively low  $A$  factor and activation energy measured for the phenoxy radical decomposition reaction support the mechanism A involving a tight intermediate.

## Introduction

There is increasing tendency in future fuels to have higher aromatic contents because partly of the change in fuel sources (such as coals and shale oils) and partly of the greater use of aromatic compounds as additives due to their high octane values.<sup>1</sup>

The chemistry of the oxidation of aromatic compounds at combustion temperatures ( $T > 1500 \text{ K}$ ) is very complex and poorly understood.<sup>2-4</sup> The present study is part of a series of experiments being carried out at NRL to elucidate the oxidation mechanism of  $C_6H_6$ , the most important benchmark system for the aromatic compounds. Recent studies of  $C_6H_6$  oxidation at high temperatures have indicated that  $C_6H_5OH$  is the most important early stage oxidation product.<sup>2-4</sup> In view of its known weak O-H bond,<sup>5</sup> the  $C_6H_5OH$  generated in the early oxidation process is expected to produce  $C_6H_5O$  very readily either unimolecularly or bimolecularly via reactions with atomic and radical species.<sup>6</sup> Additionally,  $C_6H_5O$  may also be generated by the reaction of  $C_6H_6$  with O atoms:<sup>7</sup>

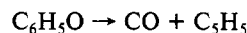
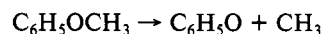


where \*<sup>†</sup> stands for the vibronically excited phenol or its precursor intermediate. We have previously reported the observation of UV emission near 250 nm in  $C_6H_6$  oxidation above 1700 K, which was attributed to the  $S_1$  state of  $C_6H_5OH$  formed by the above reaction.<sup>8</sup> The understanding of the kinetics and mechanism of the  $C_6H_5O$  radical reaction at high temperatures is therefore one of the major steps toward our ultimate goal of elucidating the complex  $C_6H_6$  oxidation chemistry.

At high temperatures, the  $C_6H_5O$  radical undergoes primarily the unimolecular decomposition reaction<sup>9,10</sup>



The rate constant for this reaction has not been accurately determined. Colussi et al. have estimated a value of  $10 \pm 5 \text{ s}^{-1}$  at 1000 K from their study of the allyl phenyl ether decomposition reaction in a VLPP reactor.<sup>9</sup> In a study recently carried out in this laboratory, we have employed a CW CO laser to monitor its decomposition kinetics using methyl phenyl ether (anisole) as a source of the  $C_6H_5O$  radical above 1000 K. Our preliminary results for the unimolecular decomposition of  $C_6H_5O$  evaluated on the basis of the two-step mechanism



have been reported elsewhere recently.<sup>6</sup>

In this article, we analyze in detail the mechanism of anisole decomposition and the effects of secondary reactions on the kinetics of the phenoxy radical decomposition process. Additionally, we have carried out a few experiments using allyl phenyl ether as the radical precursor to corroborate the measured data.

## Experimental Section

The shock tube-CO laser probing apparatus is the same as that used in previous experiments carried out in this laboratory.<sup>11,12</sup> In this work, several highly diluted mixtures of anisole and allyl phenyl ether were heated with incident shock waves. The CO formed in the decomposition reaction was detected with the 1  $\rightarrow$  0 P(10) transition of the CO laser. A detailed description of the use of stabilized CW CO lasers to measure absolute concentrations of various key combustion products, such as CO, NO, and  $H_2O$  has been given recently by Hsu and Lin.<sup>13</sup>

(1) Longwell, J. P. In "Alternate Hydrocarbon Fuels: Combustion and Chemical Kinetics"; Eds. Bowman, C. T., Birkeland, J., Eds.; American Institute of Aeronautics and Astronautics: New York, 1978; p 3.

(2) Bittner, J. D.; Howard, J. B. *Symp. (Int.) Combust.*, [Proc.], 18, 1980 **1981**, 1105.

(3) Venkat, C.; Brezinsky, K.; Glassman, I. *Symp. (Int.) Combust.*, [Proc.], 19, 1982 **1983**, 143.

(4) Bittner, J. D.; Howard, J. B.; Palmer, H. B. "NATO Conference Series, 6: Materials Science"; Plenum Press: New York, 1983; Vol. 7, p 95.

(5) McMillen, D. F.; Golden, D. M. *Annu. Rev. Phys. Chem.* **1982**, 33, 493.

(6) Lin, C.-Y.; Lin, M. C. *Int. J. Chem. Kinet.* **1985**, 17, 1025.

(7) Sibener, S. J.; Buss, R. J.; Casavecchia, P.; Hirooka, T.; Lee, Y. T. *J. Chem. Phys.* **1980**, 72, 4341.

(8) Hsu, D. S. Y.; Lin, C.-Y.; Lin, M. C. *Symp. (Int.) Combust.*, [Proc.], 20, 1984 **1985**, 623.

(9) Colussi, A. J.; Zabel, F.; Benson, S. W. *Int. J. Chem. Kinet.* **1977**, 9, 161.

(10) Harrison, A. G.; Honnen, L. R.; Dauben, H. J.; Lossing, F. P. *J. Am. Chem. Soc.* **1960**, 82, 5593.

(11) Hsu, D. S. Y.; Shaub, W. M.; Blackburn, M.; Lin, M. C. *Symp. (Int.) Combust.*, [Proc.], 19, 1982 **1983**, 89.

(12) Hsu, D. S. Y.; Shaub, W. M.; Creamer, T.; Gutman, D.; Lin, M. C. *Ber. Bunsenges. Phys. Chem.* **1983**, 87, 909.

(13) Hsu, D. S. Y.; Lin, M. C. In "Applications of Laser Chemistry and Diagnostics"; Harvey, A. B., Ed.; SPIE: Bellingham, WA, 1984; Vol. 482, p 79.

<sup>†</sup>Work performed at NRL.

<sup>‡</sup>Adjunct Professor of Chemistry, The Catholic University of America.

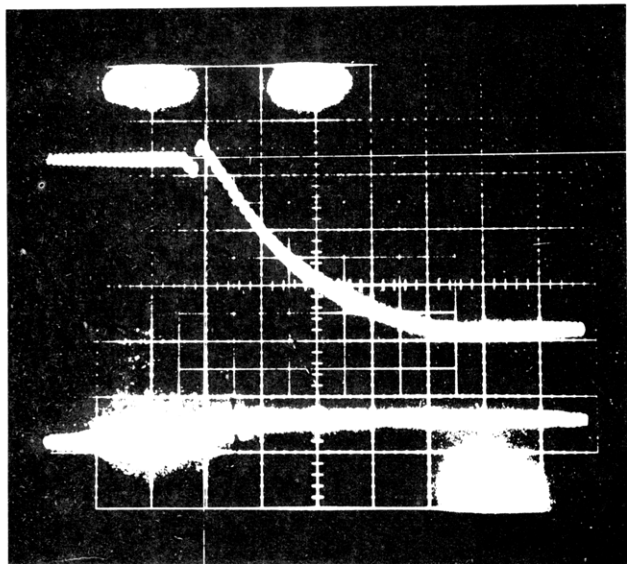


**Figure 1.** A typical CO laser absorption trace ( $T = 1321$  K,  $P = 0.535$  atm, using 0.524% anisole in Ar).

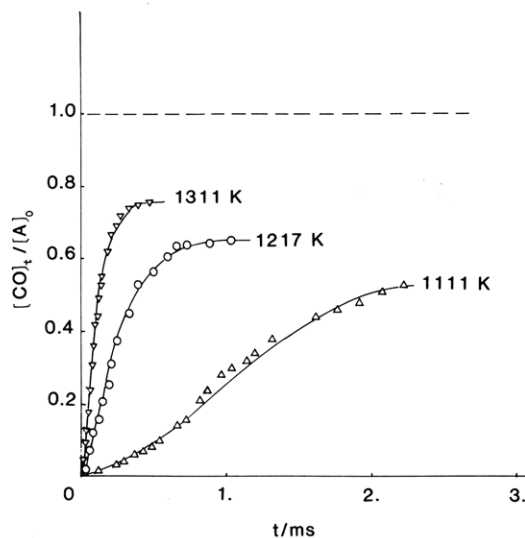


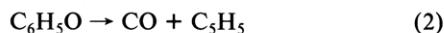
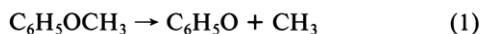
**Figure 2.** Typical relative CO production profiles: ( $\Delta$ )  $T = 1111$  K,  $P = 0.819$  atm, 0.524% anisole in Ar; ( $\circ$ )  $T = 1217$  K,  $P = 0.586$  atm, 0.758% anisole in Ar; ( $\nabla$ )  $T = 1311$  K,  $P = 0.552$  atm, 0.749% anisole in Ar.

Anisole and allyl phenyl ether, both obtained from Aldrich Chemical Co., were purified by trap-to-trap distillation prior to use. Ar (Matheson Gas Products, 99.995% pure) was used directly to prepare various mixtures.

## Results

*Approximate Evaluation of  $k_1$  and  $k_2$ .* Incident shock experiments were carried out in the temperature range from 1000 to 1580 K and the pressure range from 0.4 to 0.9 atm for six mixtures of anisole (0.108, 0.264, 0.519, 0.524, 0.749, and 0.758% in Ar) and one mixture of allyl phenyl ether (0.366% in Ar).

A typical CO absorption trace is shown in Figure 1. The absorption data were converted into CO concentration-time profiles by using the calibration method described previously.<sup>11,12</sup> Typical relative CO production profiles are shown in Figure 2. We have previously analyzed these CO formation rates during the early stage of decomposition according to the following two-step mechanism<sup>6</sup> as alluded to earlier:



On the basis of this simple scheme, the rate constants for CO

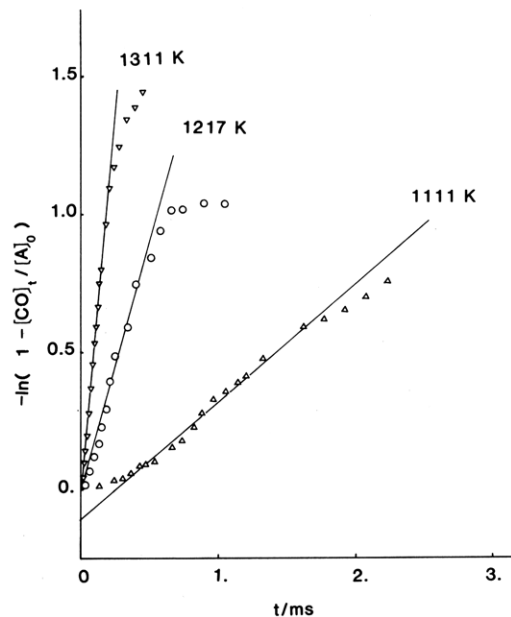


**Figure 3.**  $\ln(1 - [\text{CO}]_t/[\text{A}]_0)$  vs.  $t$  plots for same sets of data in Figure 2.

formation,  $k_2$ , can be evaluated from the slopes of  $\ln(1 - [\text{CO}]_t/[\text{A}]_0)$  vs.  $t$  plots at longer times according to the equations

$$1 - \frac{[\text{CO}]_t}{[\text{A}]_0} = \frac{k_1}{k_1 - k_2} \exp(-k_2 t) - \frac{k_2}{k_1 - k_2} \exp(-k_1 t) \quad (I)$$

and at  $T > 1200$  K

$$1 - \frac{[\text{CO}]_t}{[\text{A}]_0} = \frac{k_1}{k_1 - k_2} \exp(-k_2 t) \quad (II)$$

The approximation given by eq II is valid because reaction 1 is much faster than 2 above 1200 K as we have discussed before.<sup>6</sup> In the above equations,  $[\text{A}]_0$  is the initial concentration of anisole used. Figure 3 shows different plots of eq I for the same sets of data presented in Figure 2. The slopes of the linear portions of these plots at longer reaction times should give the values of  $k_2$  according to eq II, if the system is free from any secondary reactions which may effectively alter the concentration of the  $\text{C}_6\text{H}_5\text{O}$  radical. As will be discussed later, this assumption is only partially valid, particularly at lower temperatures ( $T < 1200$  K), because of the possible occurrence of the  $\text{CH}_3 + \text{C}_6\text{H}_5\text{O}$  reaction. The presence of this competing process is expected to lower the CO yields as manifested by the deficiency in the limiting values of CO mass balance shown in Figure 2 (i.e.,  $[\text{CO}]_{t \rightarrow \infty}/[\text{A}]_0 < 1$ ). Further discussion on this problem will be made below.

The values of the rate constants evaluated from the slopes of the linear portions of the plots shown in Figure 3, denoted by  $k_2'$ , are summarized in Figure 4 as well as in Table I together with other kinetic data. A least-squares analysis of these  $k_2'$  values gave rise to the apparent rate constant expression:

$$k_2' = 10^{11.90 \pm 0.20} \exp(-23\,900 \pm 450/T) \text{ s}^{-1} \quad (III)$$

This Arrhenius expression agrees very well with our preliminary results obtained from three sets of experiments analyzed by the same method ( $k_2' = 10^{12.0 \pm 0.2} \exp(-24\,000 \pm 690/T) \text{ s}^{-1}$ ).<sup>6</sup> It should be mentioned that the rate constants given in Figure 4 for temperatures above 1200 K have been corrected for minor pressure dependence by means of the RRKM theory using the weak collision assumption.<sup>14</sup>

According to eq I, the values of  $k_1$  at low temperatures ( $T < 1200$  K) can be estimated from the intercepts of the  $\ln(1 - [\text{CO}]_t/[\text{A}]_0)$  vs.  $t$  plots (see Figure 3). Because of the approximate nature of the mechanism assumed and the narrow (200 K) temperature range available for  $k_1$  evaluation, an accurate deter-

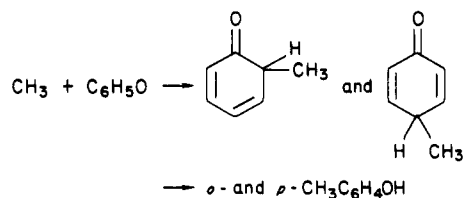
TABLE I: Experimental Data and Evaluated Rate Constants for Reactions 2 and 3

mixture <sup>a</sup>	P, atm	T, K	k <sub>2</sub> <sup>1</sup> , s <sup>-1</sup>	k <sub>2</sub> , s <sup>-1</sup>	k <sub>3</sub> , cm <sup>3</sup> ·mol <sup>-1</sup> · s <sup>-1</sup>	mixture <sup>a</sup>	P, atm	T, K	k <sub>2</sub> <sup>1</sup> , s <sup>-1</sup>	k <sub>2</sub> , s <sup>-1</sup>	k <sub>3</sub> , cm <sup>3</sup> ·mol <sup>-1</sup> · s <sup>-1</sup>
A	0.659	1186	1.2 × 10 <sup>3</sup>	1.5 × 10 <sup>3</sup>	5.0 × 10 <sup>11</sup>	C	0.585	1343	1.6 × 10 <sup>4</sup>	1.7 × 10 <sup>4</sup>	5.0 × 10 <sup>11</sup>
A	0.636	1166	1.5 × 10 <sup>3</sup>	2.1 × 10 <sup>3</sup>	3.0 × 10 <sup>11</sup>	C	0.651	1182	5.9 × 10 <sup>2</sup>	1.3 × 10 <sup>3</sup>	4.0 × 10 <sup>11</sup>
A	0.609	1159	5.1 × 10 <sup>3</sup>	6.5 × 10 <sup>3</sup>	7.0 × 10 <sup>11</sup>	C	0.499	1428	4.8 × 10 <sup>4</sup>	5.0 × 10 <sup>4</sup>	4.0 × 10 <sup>11</sup>
A	0.582	1334	1.6 × 10 <sup>4</sup>	1.9 × 10 <sup>4</sup>	7.0 × 10 <sup>11</sup>	D	0.631	1153	6.8 × 10 <sup>2</sup>	1.4 × 10 <sup>3</sup>	5.0 × 10 <sup>11</sup>
A	0.823	1192	1.7 × 10 <sup>3</sup>	2.5 × 10 <sup>3</sup>	8.0 × 10 <sup>11</sup>	D	0.819	1111	4.5 × 10 <sup>2</sup>	1.0 × 10 <sup>3</sup>	3.5 × 10 <sup>11</sup>
A	0.786	1257	5.5 × 10 <sup>3</sup>	6.0 × 10 <sup>3</sup>	7.0 × 10 <sup>11</sup>	D	0.867	1114	3.6 × 10 <sup>2</sup>	4.0 × 10 <sup>2</sup>	1.0 × 10 <sup>11</sup>
A	0.782	1149	1.4 × 10 <sup>3</sup>	2.3 × 10 <sup>3</sup>	1.0 × 10 <sup>12</sup>	D	0.927	1096	1.6 × 10 <sup>2</sup>	2.5 × 10 <sup>2</sup>	1.0 × 10 <sup>11</sup>
A	0.799	1265	5.5 × 10 <sup>3</sup>	7.5 × 10 <sup>3</sup>	4.0 × 10 <sup>11</sup>	D	0.698	1143	4.7 × 10 <sup>2</sup>	6.0 × 10 <sup>2</sup>	4.0 × 10 <sup>11</sup>
A	0.737	1318	1.1 × 10 <sup>4</sup>	1.4 × 10 <sup>4</sup>	8.0 × 10 <sup>11</sup>	D	0.727	1066	1.4 × 10 <sup>2</sup>	3.0 × 10 <sup>2</sup>	
A	0.784	1119	8.9 × 10 <sup>2</sup>	1.3 × 10 <sup>3</sup>	4.0 × 10 <sup>11</sup>	D	0.771	1066	8.3 × 10 <sup>1</sup>	2.0 × 10 <sup>2</sup>	
A	0.792	1216	3.4 × 10 <sup>3</sup>	4.5 × 10 <sup>3</sup>	5.0 × 10 <sup>11</sup>	D	0.672	1114	4.0 × 10 <sup>2</sup>	3.5 × 10 <sup>2</sup>	
A	0.567	1301	8.9 × 10 <sup>3</sup>	1.1 × 10 <sup>4</sup>	8.0 × 10 <sup>11</sup>	D	0.524	1431	4.9 × 10 <sup>4</sup>	6.5 × 10 <sup>4</sup>	6.0 × 10 <sup>11</sup>
A	0.755	1400	3.1 × 10 <sup>4</sup>	3.5 × 10 <sup>4</sup>	7.0 × 10 <sup>11</sup>	D	0.535	1321	1.2 × 10 <sup>4</sup>	1.7 × 10 <sup>4</sup>	6.0 × 10 <sup>11</sup>
A	0.645	1180	1.8 × 10 <sup>3</sup>	2.7 × 10 <sup>3</sup>	6.0 × 10 <sup>11</sup>	D	0.500	1423	4.1 × 10 <sup>4</sup>	5.5 × 10 <sup>4</sup>	8.0 × 10 <sup>11</sup>
A	0.804	1177	1.6 × 10 <sup>3</sup>	2.3 × 10 <sup>3</sup>	9.0 × 10 <sup>11</sup>	D	0.472	1431	6.1 × 10 <sup>4</sup>	6.5 × 10 <sup>4</sup>	8.0 × 10 <sup>11</sup>
A	0.809	1155	1.4 × 10 <sup>3</sup>	2.0 × 10 <sup>3</sup>	9.0 × 10 <sup>11</sup>	D	0.656	1157	5.1 × 10 <sup>2</sup>	7.5 × 10 <sup>2</sup>	4.0 × 10 <sup>11</sup>
A	0.839	1144	9.1 × 10 <sup>2</sup>	1.4 × 10 <sup>3</sup>	9.0 × 10 <sup>11</sup>	E	0.697	1062	6.0 × 10 <sup>1</sup>	1.7 × 10 <sup>2</sup>	4.0 × 10 <sup>11</sup>
B	0.658	1173	8.8 × 10 <sup>2</sup>	1.3 × 10 <sup>3</sup>	3.0 × 10 <sup>11</sup>	E	0.662	1124	2.4 × 10 <sup>2</sup>	5.0 × 10 <sup>2</sup>	4.0 × 10 <sup>11</sup>
B	0.681	1085	3.9 × 10 <sup>2</sup>	4.5 × 10 <sup>2</sup>		E	0.625	1138	4.0 × 10 <sup>2</sup>	8.0 × 10 <sup>2</sup>	5.0 × 10 <sup>11</sup>
B	0.749	1083	5.5 × 10 <sup>2</sup>	5.5 × 10 <sup>2</sup>	2.0 × 10 <sup>11</sup>	E	0.566	1151	8.4 × 10 <sup>2</sup>	1.6 × 10 <sup>3</sup>	6.0 × 10 <sup>11</sup>
B	0.619	1233	3.1 × 10 <sup>3</sup>	5.0 × 10 <sup>3</sup>	6.0 × 10 <sup>11</sup>	E	0.595	1268	3.0 × 10 <sup>3</sup>	4.5 × 10 <sup>3</sup>	7.0 × 10 <sup>11</sup>
B	0.584	1345	1.8 × 10 <sup>4</sup>	2.3 × 10 <sup>4</sup>	6.0 × 10 <sup>11</sup>	E	0.693	1017	3.5 × 10 <sup>1</sup>	1.2 × 10 <sup>2</sup>	2.0 × 10 <sup>11</sup>
B	0.587	1299	1.3 × 10 <sup>4</sup>	1.5 × 10 <sup>4</sup>	6.0 × 10 <sup>11</sup>	E	0.552	1311	5.5 × 10 <sup>3</sup>	7.5 × 10 <sup>3</sup>	6.5 × 10 <sup>11</sup>
B	0.559	1391	3.1 × 10 <sup>4</sup>	3.3 × 10 <sup>4</sup>	8.0 × 10 <sup>11</sup>	E	0.508	1403	2.2 × 10 <sup>4</sup>	3.0 × 10 <sup>4</sup>	7.0 × 10 <sup>11</sup>
B	0.491	1470	7.0 × 10 <sup>4</sup>	1.0 × 10 <sup>5</sup>	8.0 × 10 <sup>11</sup>	F	0.653	1162	5.3 × 10 <sup>2</sup>	1.0 × 10 <sup>3</sup>	7.0 × 10 <sup>11</sup>
B	0.684	1131	6.0 × 10 <sup>2</sup>	8.0 × 10 <sup>2</sup>	1.0 × 10 <sup>11</sup>	F	0.726	1038	6.9 × 10 <sup>1</sup>	1.5 × 10 <sup>2</sup>	
B	0.493	1586	1.2 × 10 <sup>5</sup>	1.2 × 10 <sup>5</sup>	4.0 × 10 <sup>11</sup>	F	0.745	1015	2.8 × 10 <sup>1</sup>	1.5 × 10 <sup>2</sup>	4.0 × 10 <sup>11</sup>
B	0.514	1361	3.3 × 10 <sup>4</sup>	3.0 × 10 <sup>4</sup>	2.0 × 10 <sup>11</sup>	F	0.724	1072	1.0 × 10 <sup>2</sup>	2.3 × 10 <sup>2</sup>	4.0 × 10 <sup>11</sup>
B	0.639	1190	2.0 × 10 <sup>3</sup>	3.0 × 10 <sup>3</sup>	8.0 × 10 <sup>11</sup>	F	0.692	1131	3.3 × 10 <sup>2</sup>	5.0 × 10 <sup>2</sup>	2.0 × 10 <sup>11</sup>
B	0.658	1129	8.8 × 10 <sup>2</sup>	1.0 × 10 <sup>3</sup>		F	0.586	1217	2.1 × 10 <sup>3</sup>	3.3 × 10 <sup>3</sup>	9.0 × 10 <sup>11</sup>
C	0.631	1186	1.4 × 10 <sup>3</sup>	2.4 × 10 <sup>3</sup>	7.0 × 10 <sup>11</sup>	F	0.568	1336	8.4 × 10 <sup>3</sup>	1.0 × 10 <sup>4</sup>	5.0 × 10 <sup>11</sup>
C	0.599	1347	1.0 × 10 <sup>4</sup>	1.2 × 10 <sup>4</sup>	9.0 × 10 <sup>11</sup>	F	0.494	1361	1.7 × 10 <sup>4</sup>	2.3 × 10 <sup>4</sup>	9.0 × 10 <sup>11</sup>
C	0.520	1430	4.0 × 10 <sup>4</sup>	4.0 × 10 <sup>4</sup>	6.0 × 10 <sup>11</sup>	F	0.475	1491	5.4 × 10 <sup>4</sup>	6.6 × 10 <sup>4</sup>	4.0 × 10 <sup>11</sup>
C	0.655	1146	3.4 × 10 <sup>2</sup>	1.2 × 10 <sup>3</sup>	8.0 × 10 <sup>11</sup>	F	0.439	1486	6.5 × 10 <sup>4</sup>	7.5 × 10 <sup>4</sup>	6.0 × 10 <sup>11</sup>
C	0.643	1201	1.1 × 10 <sup>3</sup>	1.6 × 10 <sup>3</sup>	5.5 × 10 <sup>11</sup>	F	0.704	1038	6.1 × 10 <sup>1</sup>	2.3 × 10 <sup>2</sup>	1.0 × 10 <sup>11</sup>
C	0.612	1234	2.4 × 10 <sup>3</sup>	3.0 × 10 <sup>3</sup>	3.0 × 10 <sup>11</sup>	F	0.498	1427	3.6 × 10 <sup>4</sup>	3.6 × 10 <sup>4</sup>	3.0 × 10 <sup>11</sup>
C	0.595	1293	1.1 × 10 <sup>4</sup>	1.1 × 10 <sup>4</sup>	3.0 × 10 <sup>11</sup>						

<sup>a</sup> Mixture A: 0.108%; anisole in Ar; mixture B: 0.264% anisole in Ar; mixture C: 0.519% anisole in Ar; mixture D: 0.524% anisole in Ar; mixture E: 0.749% anisole in Ar; mixture F: 0.758% anisole in Ar.

mination of the Arrhenius parameters for anisole decomposition (which is not available in the literature) is not possible. However, these approximate rate constants are useful as starting values for modeling CO formation profiles in the very early stage of anisole decomposition at low temperatures. The values of  $k_1$  summarized in Table II for 24 sets of data have been slightly adjusted to fit exactly the observed early CO profiles. From these rate constants we can evaluate the frequency factor using the Arrhenius equation:  $A_1 = k_1/\exp(-E_1/RT)$ , where  $E_1 \approx \Delta H_1^\circ + RT = 65.8$  kcal/mol, taking  $\Delta H_1^\circ = 63.8$  kcal/mol.<sup>5</sup> The average of the 24  $A_1$  values summarized in Table II gave rise to  $A_1 = (1.2 \pm 0.3) \times 10^{16}$  s<sup>-1</sup>. At 1000 K, the value of  $k_1 = 50$  s<sup>-1</sup> estimated by  $k_1 = 1.2 \times 10^{16} \exp(-65800/RT)$  s<sup>-1</sup> can be compared with that for the decomposition of ethyl phenyl ether in the high-pressure limit determined by Colussi et al.,<sup>9</sup> 126 s<sup>-1</sup>.

**Evaluation of  $k_2$  and  $k_3$  by Kinetic Modeling.** The deficiency in CO mass balance mentioned before is believed to result from the  $\text{CH}_3 + \text{C}_6\text{H}_5\text{O}$  reaction which can competitively remove the phenoxy radical. This reaction has been previously shown to form *o*- and *p*-cresols via methylcyclohexadienones by Mulcahy and Williams.<sup>15,16</sup>



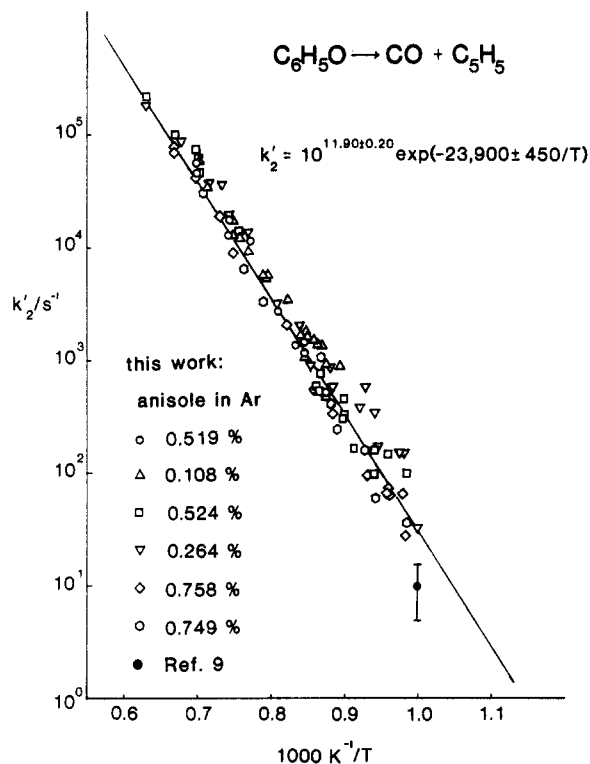
(15) Mulcahy, M. F. R.; Williams, D. J. *Nature* 1963, 199, 761.

TABLE II: Estimated First-Order Rate Constants for Anisole Decomposition

mixture <sup>a</sup>	P, atm	T, K	k <sub>1</sub> , s <sup>-1</sup>	A <sub>1</sub> , <sup>b</sup> s <sup>-1</sup>
B	0.684	1131	2.9 × 10 <sup>3</sup>	1.5 × 10 <sup>16</sup>
B	0.749	1083	7.9 × 10 <sup>2</sup>	1.5 × 10 <sup>16</sup>
B	0.681	1085	8.3 × 10 <sup>2</sup>	1.5 × 10 <sup>16</sup>
C	0.655	1146	4.2 × 10 <sup>3</sup>	1.5 × 10 <sup>16</sup>
C	0.651	1182	1.0 × 10 <sup>4</sup>	1.5 × 10 <sup>16</sup>
C	0.631	1186	1.1 × 10 <sup>4</sup>	1.5 × 10 <sup>16</sup>
D	0.672	1114	1.2 × 10 <sup>3</sup>	9.8 × 10 <sup>15</sup>
D	0.727	1066	3.2 × 10 <sup>2</sup>	9.9 × 10 <sup>15</sup>
D	0.771	1066	3.3 × 10 <sup>2</sup>	1.0 × 10 <sup>16</sup>
D	0.698	1143	2.6 × 10 <sup>3</sup>	1.0 × 10 <sup>16</sup>
D	0.819	1111	1.1 × 10 <sup>3</sup>	9.8 × 10 <sup>15</sup>
D	0.867	1114	1.2 × 10 <sup>3</sup>	9.8 × 10 <sup>15</sup>
D	0.927	1096	7.6 × 10 <sup>2</sup>	1.0 × 10 <sup>16</sup>
D	0.631	1154	3.7 × 10 <sup>3</sup>	1.1 × 10 <sup>16</sup>
E	0.693	1017	1.4 × 10 <sup>2</sup>	2.0 × 10 <sup>16</sup>
E	0.697	1062	2.8 × 10 <sup>2</sup>	9.8 × 10 <sup>15</sup>
E	0.566	1151	4.8 × 10 <sup>3</sup>	1.5 × 10 <sup>16</sup>
E	0.662	1124	1.6 × 10 <sup>3</sup>	9.9 × 10 <sup>15</sup>
E	0.625	1138	3.0 × 10 <sup>3</sup>	1.3 × 10 <sup>16</sup>
F	0.745	1015	1.2 × 10 <sup>2</sup>	1.8 × 10 <sup>16</sup>
F	0.724	1072	3.9 × 10 <sup>2</sup>	1.0 × 10 <sup>16</sup>
F	0.704	1038	1.4 × 10 <sup>2</sup>	1.0 × 10 <sup>16</sup>
F	0.726	1038	1.4 × 10 <sup>2</sup>	1.0 × 10 <sup>16</sup>
F	0.692	1131	1.9 × 10 <sup>3</sup>	9.9 × 10 <sup>15</sup>

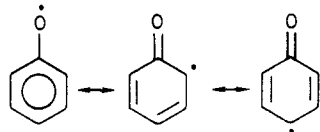
<sup>a</sup> For mixture composition, see the footnote for Table I. <sup>b</sup>  $A_1 = k_1/\exp(-65800/RT)$ ; averaged value of  $A_1 = (1.2 \pm 0.3) \times 10^{16}$ .

The occurrence of this reaction can account for the formation of cresols in the pyrolysis of anisole at lower temperatures.<sup>17,18</sup> The



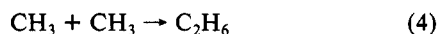
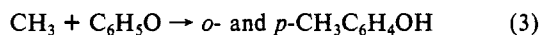
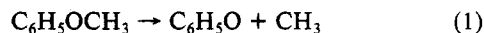
**Figure 4.** Arrhenius plot for  $k_2'$  (see the comment given in the caption for Figure 8 on the low-pressure value of  $k_2$  reported in ref 9).

above combination mechanism is quite reasonable in view of the possible existence of the following resonance structures:<sup>15,16</sup>



The cresols thus formed are thermochemically much more stable than anisole and the phenoxy radical. Accordingly, their formation depletes the yield of CO, leading to the apparent loss of CO and thus the deviation from linearity in the  $\ln(1 - [\text{CO}]_t/[\text{A}]_0)$  vs.  $t$  plots as shown in Figure 3.

To correct the effects of this side reaction, we have attempted to computer-model the production of CO using the following mechanism:



The modeling could be readily done by varying  $k_3$  (which is not known) to fit the observed  $[\text{CO}]_t/[\text{A}]_0$  values at long reaction times and simultaneously fine-tuning the values of  $k_2$ , which were initially set as  $k_2'$ , to account for the rising portions of the CO formation profiles. The values of  $k_1$  obtained from the preceding section,  $k_1 = 1.2 \times 10^{16} \exp(-65800/RT) \text{ s}^{-1}$ , and  $k_4$  by Glänzer et al.<sup>19</sup> with appropriate pressure dependence corrections were used without adjustment. The simple kinetic modeling quickly led to convergence in the values of  $k_2$  and  $k_3$  because the corrections for the observed deviations in CO yields from those predicted by the two-step scheme presented in the preceding section are usually not very large at low temperatures and were found to be quite

(16) Mulcahy, M. F. R.; Williams, D. J. *Aust. J. Chem.* **1965**, *18*, 20.

(17) Kislitsyn, A. N.; Savinykh, V. I.; Latysheva, V. A. *Zh. Prikl. Khim.* **1972**, *45*, 384.

(18) Bredenbergh, J. B.; Ceylan, R. *Fuel* **1983**, *62*, 342.

(19) Glänzer, K.; Quack, M.; Troe, J. *Chem. Phys. Lett.* **1976**, *39*, 304.

(20) Mulcahy, M. F. R.; Tucker, B. G.; Williams, D. J.; Wilmshurst, J. R. *Aust. J. Chem.* **1967**, *20*, 1155.

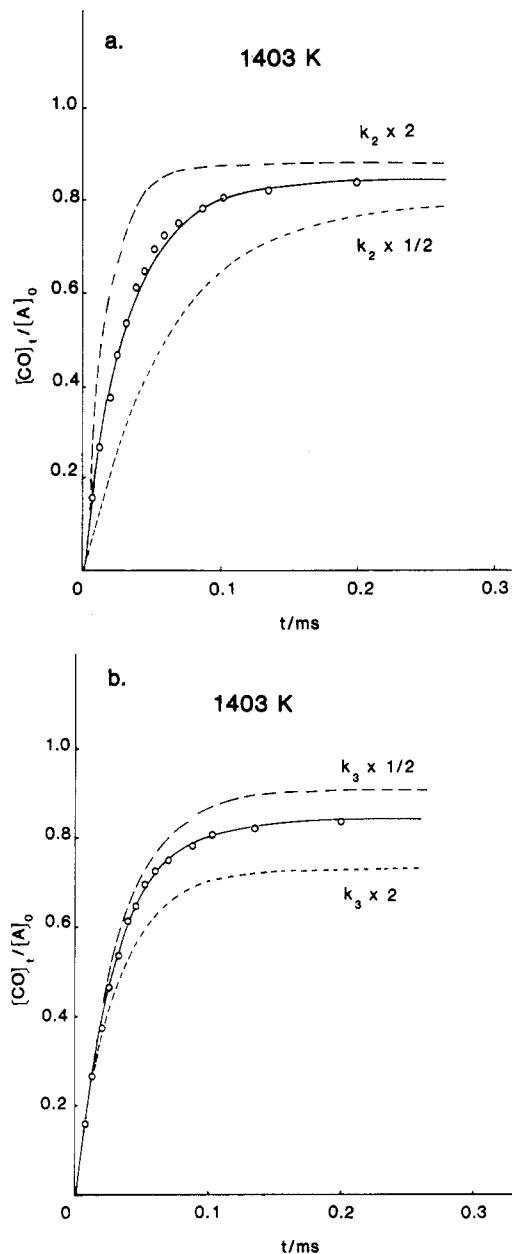


**Figure 5.** Observed and modeled CO production profiles at 1403 K for 0.749% anisole/Ar mixture at  $P = 0.508$  atm: (O) experimental results; (—) modeled result using the mechanism including reactions 1–4; (---) sensitivity tests for  $k_2$  (a) and  $k_3$  (b). The test results clearly show that the computed CO yield in the rising portion of the production profile depends much more sensitively on the value of  $k_2$  than  $k_3$ , whereas the CO yield in the plateau region at longer reaction times varies more strongly with  $k_3$  than  $k_2$ . These effects facilitate the convergency of  $k_2$  and  $k_3$  immensely.

small above 1200 K, at which reaction 2 becomes very fast. Some of the modeled data are shown in Figures 5–7, together with the results of sensitivity tests for  $k_2$  and  $k_3$ .

The values of  $k_2$  and  $k_3$  derived from kinetic modeling are summarized in Table I. The Arrhenius plot for  $k_2$  is presented in Figure 8. The least-squares analysis of  $k_2$ , after minor corrections for pressure effect at high temperatures, led to the following expression,

$$k_2 = 10^{11.40 \pm 0.20} \exp(-22100 \pm 450/T) \text{ s}^{-1} \quad (\text{IV})$$

The slightly lower values for the  $A$  factor and  $E_a$ , in comparison with those given in eq III, result essentially from the slightly increased value of  $k_2$  below 1200 K where the effect of reaction 3 is larger.

The values of  $k_3$  fall in the range of  $(1\text{--}10) \times 10^{11} \text{ cm}^3 \cdot \text{mol}^{-1} \cdot \text{s}^{-1}$  with the averaged value of  $(5.5 \pm 2.0) \times 10^{11} \text{ cm}^3 \cdot \text{mol}^{-1} \cdot \text{s}^{-1}$ , which

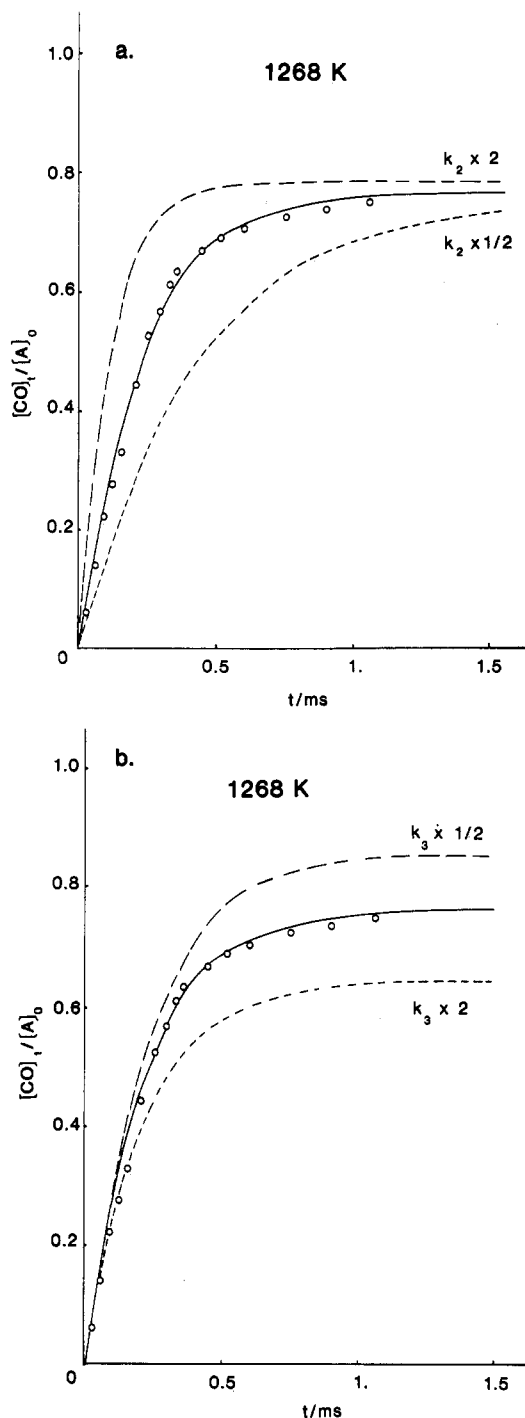


Figure 6. Observed and modeled CO production profiles at 1268 K for 0.749% anisole/Ar mixture at  $P = 0.595$  atm; symbols are the same as those in Figure 5.

seems reasonable for such a combination reaction. Further analysis of this mechanistically very interesting reaction is still under way.

Aside from reactions 3 and 4 included in the above mechanism, we have also tested the possible influence of the following reactions on CO formation, including the reverse of reaction 2:

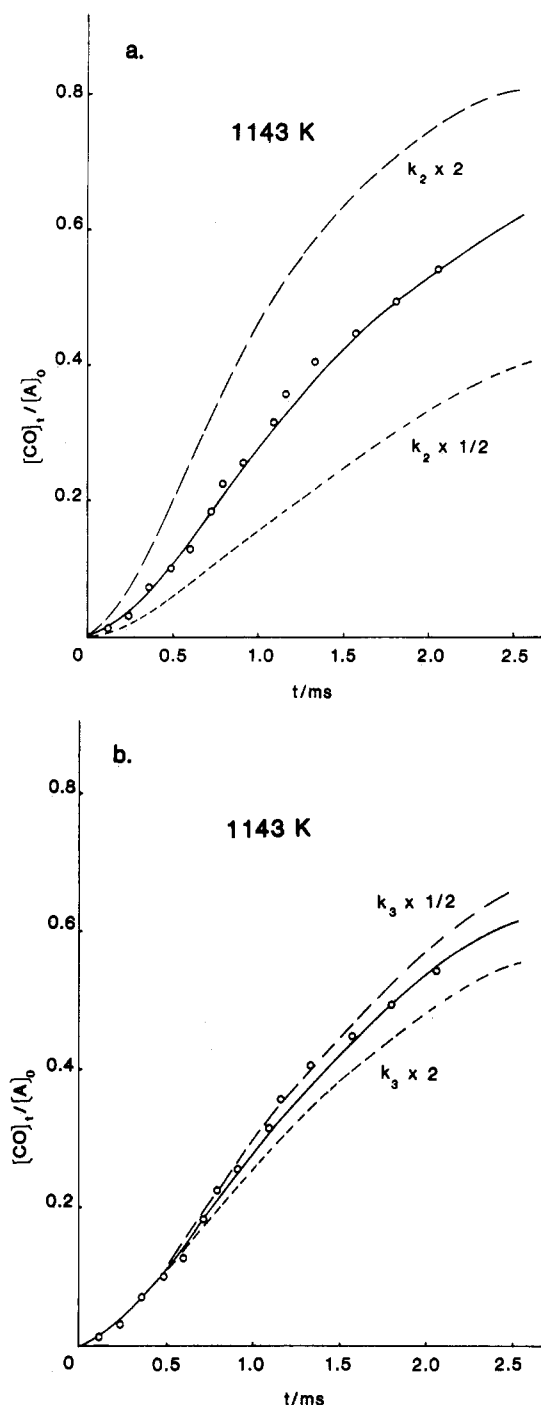
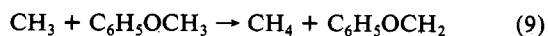
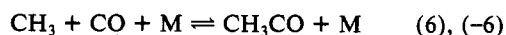
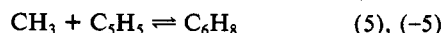
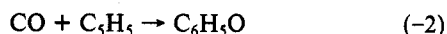


Figure 7. Observed and modeled CO production profiles at 1143 K for 0.524% anisole/Ar mixture of  $P = 0.698$  atm; symbols are the same as those in Figure 5.

These processes were, however, found to have very minor effects on the observed CO formation profiles particularly at temperatures above 1200 K. The rate constants for reactions -2 and -5 were estimated by the equilibrium constants calculated from the known thermochemistry of  $\text{C}_5\text{H}_5$  and group additivity rules.<sup>21</sup> They are summarized in Table III together with other rate constants used in the modeling calculations.

#### Discussion

The observed CO production profiles from six different, highly diluted mixtures of anisole (0.1–0.75% in Ar) in the temperature range of 1000–1580 K could be quantitatively accounted for with the mechanism consisting of reactions 1–4. Reaction 2 is believed to be the sole source of CO. It is responsible for nearly all of the

(21) Benson, S. W. "Thermochemical Kinetics"; Wiley: New York, 1976.

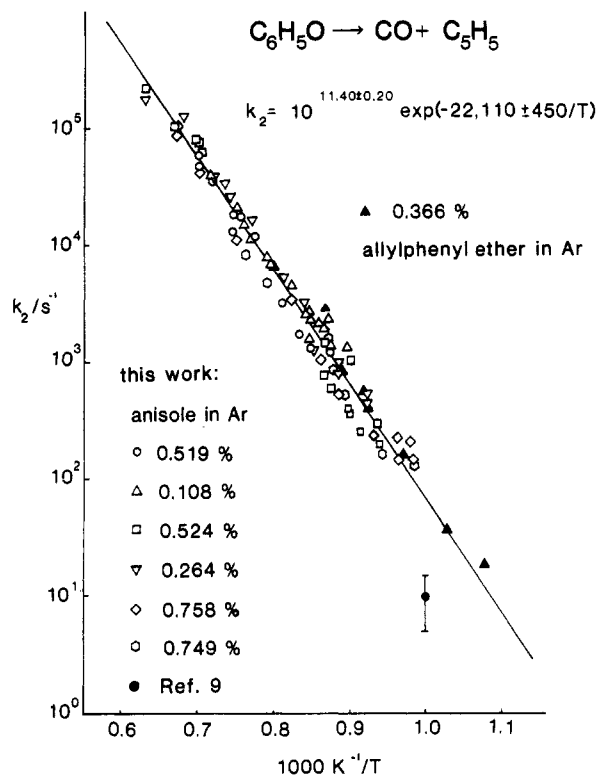


**Figure 8.** Arrhenius plot for  $k_2$ . The Arrhenius expression,  $k_2 = 10^{11.40 \pm 0.20} \exp(-22\,100 \pm 450/T) \text{ s}^{-1}$ , was obtained from the least-squares analyses of data from six different mixtures of anisole in Ar. The lower value of  $k_2$  from ref 9 by Colussi et al. was apparently due to pressure effect. The extrapolation of our high-pressure value at 1000 K to the VLPP conditions employed in ref 9 led to a value of  $12.7 \text{ s}^{-1}$  which agrees with their value of  $10 \pm 5 \text{ s}^{-1}$ .

**TABLE III: Rate Constants Used in the Kinetic Modeling of CO Production,  $k = AT^n \exp(-E/RT)^a$**

reaction	A	n	E	remarks
1	$1.2 \times 10^{16}$	0	65.8	this work, see text
2	$2.5 \times 10^{11}$	0	44.0	this work, see text
-2	$8.6 \times 10^8$	0	26.9	calcd from $k_2$ and $K_2^b$
3	$(1-10) \times 10^{11}$	0	0	this work, see text
4	$(2-5) \times 10^{12}$	0	0	ref 19, depending on pressure
5	$1.0 \times 10^{12}$	0	0	assumed
-5	$4.8 \times 10^{14}$	0	58.5	calcd from $k_5$ and $K_5^c$
6	$1.2 \times 10^{23}$	-2.8	7.6	d
-6	$1.9 \times 10^{22}$	-1.7	16.7	d
7	$2.4 \times 10^{13}$	0	0	d
8	$1.0 \times 10^{12}$	0	0	assumed
9	$5.0 \times 10^{11}$	0	10.5	ref 20
10	$3.2 \times 10^{12}$	0	21.0	ref 20

<sup>a</sup> A in  $\text{cm}^3$ , mol, and s units, E in kcal/mol. <sup>b</sup>  $K_2 = 2.9 \times 10^2 \exp(-17\,100/RT) \text{ mol} \cdot (\text{cm}^3)^{-1}$ . <sup>c</sup>  $K_5 = 2.1 \times 10^{-3} \exp(58\,500/RT) \text{ cm}^3 \cdot \text{mol}^{-1}$ . <sup>d</sup> Based on a recent compilation and recommendation by W. Tsang.

phenoxy radical disappearance rates above 1200 K. The limiting CO yields,  $[\text{CO}]_{\infty}$ , however, were always found to be less than the starting concentrations of anisole,  $[\text{A}]_0$ . This deficiency in CO mass balance was attributed to the occurrence of reaction 3, which has previously been shown to produce *o*- and *p*-cresols,  $\text{CH}_3\text{C}_6\text{H}_4\text{OH}$ . Since cresols are thermochemically much more stable than both anisole and the phenoxy radical, their production at lower temperatures (at which the  $\text{C}_6\text{H}_5\text{O}$  decomposition reaction is comparably slow) effectively reduces the yield of CO as was experimentally observed.

Kinetic modeling of CO production profiles based on the above relatively simple scheme led to

$$k_2 = 10^{11.40 \pm 0.20} \exp(-22\,100 \pm 450/T) \text{ s}^{-1}$$

$$k_3 = (5.5 \pm 2.0) \times 10^{11} \text{ cm}^3 \cdot \text{mol}^{-1} \cdot \text{s}^{-1}$$

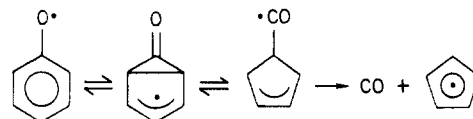
covering the temperature range of 1000–1580 K. For  $k_2$  the slight pressure effect, which is more pronounced at the high-temperature end, has been corrected by means of the RRKM theory based on the weak collision model.<sup>14</sup>

To corroborate the measured  $\text{C}_6\text{H}_5\text{O}$  decomposition rates, particularly for the lower temperature end of this study ( $T \leq 1100 \text{ K}$ ) which is subject to a slightly larger uncertainty because of the  $\text{CH}_3 + \text{C}_6\text{H}_5\text{O}$  reaction, we have employed allyl phenyl ether as the source of  $\text{C}_6\text{H}_5\text{O}$  radicals. The much lower activation energy for  $\text{C}_6\text{H}_5\text{O}$  production from this source<sup>9</sup> and the lower reactivity of the allyl radical in comparison with  $\text{CH}_3$  allow us to extend the temperature down to 900 K. The results obtained from the decomposition of the 0.366% allyl phenyl ether/Ar mixture in incident shocks are included in Figure 8 for comparison. These data are seen to be in full agreement with those obtained from anisole decomposition. It should be mentioned that the  $[\text{CO}]_{\infty}/[\text{A}]_0$  ratios measured at higher temperatures were found to be scattered around unity, suggesting that the recombination of  $\text{C}_6\text{H}_5\text{O}$  with  $\text{C}_3\text{H}_5$  is comparatively unimportant. Further study of this reaction system seems to be worthwhile, especially using a heated shock tube (to alleviate the low vapor pressure problem associated with the system).

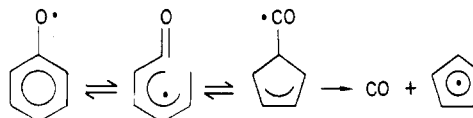
The values of  $k_3$  summarized in Table II were within the range of  $(1-10) \times 10^{11} \text{ cm}^3 \cdot \text{mol}^{-1} \cdot \text{s}^{-1}$ . The activation energy for the recombination process,  $\text{CH}_3 + \text{C}_6\text{H}_5\text{O}$ , could not be reliably determined due to the scatter of the data. The values of  $k_3$  appear to be reasonable for this type of process involving the rather unreactive  $\text{C}_6\text{H}_5\text{O}$  radical. Currently, we are in the process of analyzing the mechanism of this interesting reaction (which involves 1,3-sigmatropic hydrogen transfer) using the formulation put forward by us previously on the basis of the RRKM theory to account for the kinetics of high-temperature processes that occur via long-lived intermediates.<sup>12,22</sup> The results of this analysis will be discussed in a separate report.

The relatively small frequency factor ( $2.5 \times 10^{11} \text{ s}^{-1}$ ) and activation energy ( $44.0 \pm 0.9 \text{ kcal/mol}$ ) for the unimolecular decomposition of the  $\text{C}_6\text{H}_5\text{O}$  radical determined here is most interesting. Benson and co-workers<sup>9</sup> have previously proposed two possible mechanisms to account for the formation of CO and  $\text{C}_3\text{H}_5$ :

Mechanism A:



Mechanism B:



They favored mechanism A on the basis of the estimated  $k_2$  at 1000 K and on other thermochemical grounds. The apparent low  $A$  factor and activation energy measured in this study seem to render a very strong support for this tight-complex mechanism. The alternate mechanism B would perhaps require a much larger activation energy, together with a "normal"  $A$  factor of  $\geq 10^{13.5} \text{ s}^{-1}$ , for the ring-opening process.

## Conclusion

The kinetics of the unimolecular reaction of the  $\text{C}_6\text{H}_5\text{O}$  radical has been investigated in a shock tube using a stabilized CO laser to monitor the production of CO. Both anisole and allyl phenyl ether were employed as phenoxy radical sources. The kinetic modeling of observed CO production profiles obtained from about 70 sets of experiments covering 1000–1580 K gave rise to the rate constants

$$k_2 = 10^{11.40 \pm 0.20} \exp(-22\,100 \pm 450/T) \text{ s}^{-1}$$

$$k_3 = (5.5 \pm 2.0) \times 10^{11} \text{ cm}^3 \cdot \text{mol}^{-1} \cdot \text{s}^{-1}$$

for the unimolecular decomposition of  $\text{C}_6\text{H}_5\text{O}$  and the reaction of  $\text{CH}_3$  with  $\text{C}_6\text{H}_5\text{O}$ , respectively. The relatively low values of the  $A$  factor and activation energy for the  $\text{C}_6\text{H}_5\text{O}$  decomposition reaction favor the mechanism that involves a bicyclic radical intermediate. Additionally, the modeling of CO yields in the very early stage of anisole decomposition at temperatures below 1200

K gave rise to the following approximate rate constant for the unimolecular decomposition process:

$$k_1 \approx (1.2 \pm 0.3) \times 10^{16} \exp(-33\,100/T) \text{ s}^{-1}$$

The rate constant determined hereon for this important process is expected to be useful for the interpretation of the complex  $\text{C}_6\text{H}_6$  combustion chemistry.

Registry No.  $\text{C}_6\text{H}_5\text{OCH}_3$ , 100-66-3.

## The Elimination Kinetics of Methoxyalkyl Chlorides in the Gas Phase. Evidence for Neighboring Group Participation

Gabriel Chuchani\* and Ignacio Martin

Centro de Química, Instituto Venezolano de Investigaciones Científicas, Apartado 1827, Caracas 1010-A, Venezuela (Received: July 22, 1985)

The rates of elimination of 3-methoxy-1-chloropropane and 4-methoxy-1-chlorobutane have been determined in a seasoned, static reaction vessel over the temperature range of 410–490 °C and the pressure range of 56–181 torr. The reactions are homogeneous and unimolecular, follow a first-order rate law, and are invariant to the presence of a twofold or greater excess of the radical chain inhibitor toluene. The overall rate coefficients are given by the following Arrhenius equations: for 3-methoxy-1-chloropropane,  $\log k_1 (\text{s}^{-1}) = (12.92 \pm 0.48) - (226.0 \pm 6.8) \text{ kJ mol}^{-1} (2.303RT)^{-1}$ ; for 4-methoxy-1-chlorobutane,  $\log k_1 (\text{s}^{-1}) = (12.89 \pm 0.26) - (218.1 \pm 3.5) \text{ kJ mol}^{-1} (2.303RT)^{-1}$ . The  $\text{CH}_3\text{O}$  group in 4-methoxy-1-chlorobutane has been found to assist anchimerically the elimination reaction, where dehydrochlorination and tetrahydrofuran formation arise from an intimate ion pair type of mechanism. The partial rates for these parallel eliminations have been determined and reported. Participation of the  $\text{CH}_3\text{O}$  in 3-methoxy-1-chloropropane is barely detected. The present results give further evidence of intimate ion pair mechanism through neighboring group participation in the gas-phase elimination of certain types of organic molecules.

### Introduction

An intimate ion pair mechanism in the gas-phase pyrolysis of certain types of organic halides is thought to occur by way of neighboring group participation.<sup>1</sup> This phenomenon may arise whereby a substituent located in the same molecule assists in the stabilization of the reaction center in the transition state. In some cases, the participating atom of a substituent may form an irreversible or real bond whereby a leaving atom possibly migrates or rearranges through an intramolecular solvation or autosolvation in the intimate ion pair type of mechanism. In order to observe neighboring group participation in gas-phase reactions, according to our recent proposed generalization,<sup>2</sup> it is necessary that (a) the transition state be very polar, (b) the participating atom be large and able to overlap, and (c) the participating atom be highly polarizable.

The  $\text{CH}_3\text{O}$  substituent in the gas-phase elimination of  $\text{CH}_3\text{O}(\text{CH}_2)_n\text{OAc}$  ( $n = 2, 3, 4$ )<sup>3</sup> does not provide anchimeric assistance as does the  $(\text{CH}_3)_2\text{N}$  substituent in the gas-phase elimination of  $(\text{CH}_3)_2\text{N}(\text{CH}_2)_n\text{OAc}$  ( $n = 2, 3, 4$ ).<sup>4</sup> These results suggest that the oxygen atom is not as polarizable as the nitrogen atom, and, moreover, the transition state of ester pyrolysis is not very polar. However, since the pyrolysis of alkyl halides in the gas phase are more heterolytic in nature than esters,<sup>5</sup> the present work is aimed at studying the influence and possible participation of the  $\text{CH}_3\text{O}$

substituent in the gas-phase pyrolysis of  $\text{CH}_3\text{O}(\text{CH}_2)_n\text{Cl}$ , where  $n = 2, 3$ , and 4.

### Experimental Section

**3-Methoxy-1-chloropropane.** 3-Methoxy-1-propanol (K & K, Labs) was added to  $\text{PCl}_3$  in pyridine as described<sup>7</sup> (bp 103 °C at 630 torr; lit. bp 110.4 °C at 756.6 torr<sup>7</sup>). The chloro ether was distilled to 97% purity as determined by GLC (FFAP 7%, Chromosorb G AW DMCS 80–100 mesh and Silicone DC 200/100, Chromosorb W AW DMCS 80–100 mesh). The pyrolysis intermediate, allylmethyl ether, was prepared by treating allyl bromide with  $\text{CH}_3\text{ONa}$  in  $\text{CH}_3\text{OH}$  (bp 36 °C at 630 torr; lit. bp 46 °C at 760 torr<sup>8</sup>) and analyzed by using the FFAP column. Trimethylene oxide (Aldrich), propene (Matheson), and formaldehyde from 1,3,5-trioxane (Aldrich) were analyzed with a Porapak Q 80–100 mesh and Carbosieve B 60–80 mesh.

**4-Methoxy-1-chlorobutane.** Treatment of 4-methoxy-1-butanol (Sapon Lab.) with  $\text{PCl}_3$  in pyridine yielded the corresponding chloro ether<sup>7</sup> (bp 135–136 °C at 630 torr; lit. bp 142.5–142.8 °C at 760 torr<sup>7</sup>). This compound was distilled several times and a fraction of 98.7% purity (GLC, same FFAP column) was used. Tetrahydrofuran (Merck) was analyzed on the FFAP column, while  $\text{CH}_3\text{Cl}$  (Matheson) was analyzed on a Porapak Q 80–100 mesh column. 4-Methoxy-1-butene was prepared by pyrolyzing 4-methoxybutyl acetate as reported<sup>3</sup> and 4-methoxy-2-butene was prepared from isomerization of 4-methoxy-1-butene with HCl in the gas phase. Both olefinic ethers were analyzed on the FFAP columns.

(1) Chuchani, G.; Dominguez, R. M. *Int. J. Chem. Kinet.* **1983**, *15*, 795.

(2) Chuchani, G.; Martin, I.; Martin, G.; Bigley, D. B. *Int. J. Chem. Kinet.* **1979**, *11*, 109.

(3) Chuchani, G.; Rotinov, A. *React. Kinet. Catal. Lett.* **1978**, *9*, 359.

(4) Chuchani, G.; Rotinov, A.; Dominguez, R. M.; González, N. *J. Org. Chem.* **1984**, *49*, 4157.

(5) Maccoll, A. *Chem. Rev.* **1969**, *69*, 33.

(6) Kwart, H.; Sarnier, S. F.; Slutsky, J. *J. Am. Chem. Soc.* **1973**, *95*, 5234.

(7) Palomaa, M. H.; Jansson, R. *Berichte* **1931**, *64*, 1606.

(8) Bailey, W.; Nicholas, L. *J. Org. Chem.* **1956**, *21*, 648.